ISSN No:-2456-2165

A Hybrid Maximum Power Point Tracking System for Electrical Power Distributed System in a AL-Fajer Nano Satellite

Harith M. Jasim
Dept. of Electrical Engineering
Ministry of the Interior
Baghdad, Iraq

Abstract:- Many institutions have embraced the nano satellite standard as an economical means of doing space science from its inception, with the supply of electrical power to the nano satellites serving as the backbone of any such mission. This study describes the design of a solar arrays, batteries based power system that uses peak power trackers to regulate solar arrays and charge batteries. As a measure of redundancy, the peak power tracking is conducted by an active search algorithm, Perturb & Observe, in both analog and digital form. Mathematical analysis, numerical modeling, and experimental data are used to validate the suggested strategy. All of this demonstrates the correctness of the proposal, which yielded a good overall system performance.

Keywords:- *nano; nano sattlite; Electrical power supply; maximum power point tracking; solar array.*

I. INTRODUCTION

Designing, producing, and finally launching a nano satellite to perform space science and exploration has always been a costly endeavor, one that most colleges cannot afford. Since the establishment of the nano satellite design specification in the year 1999 by aerospace engineering professors Jordi Puig-Sauri (from California Polytechnic State University) and Robert Twiggs [1], this scenario has all but changed. They realized that a low volume, lightweight nanosatellite, deployable from a standardized deployed (named a P-POD, Poly Picosatellite Orbital Deployed) that easily interacts with launch vehicles was required to reduce design and, in particular, launch costs. As a result, the conventional CubeSat is only 10x10x10cm in size and can only weigh 1.33kg. It is assumed that these and other satellites require electrical power to function and complete their missions. The provision of electrical power to space vehicles is likely the most basic requirement of the satellite payload, with failure of the power system inevitably resulting in the failure of the space mission [2].

This research commences with an overview of nano satellite power systems, together with primary and secondary electrical power sources. Top level design then discusses different electrical power system topologies together with the design and test results of the maximum power tracker. As shown in Figure 1, a nano satellite's electrical power system generate, stores, manages, and delivers electrical power to the all nano satellite's electrical system. The payload demands for average and peak electrical power, as well as the orbital profile, are important sizing factors affecting the solar array and battery unit, and must take into account power demands at the beginning and end of life in order for the electrical power system to perform all of its top-level functions. Top-level functions include providing a constant source of electrical power to the satellite bus for the duration of the mission, controlling and distributing power to the satellite, providing power during periods of average and peak power demand, protecting against bus faults, and monitoring and communicating electrical power system health and status to the on-board microcontroller.

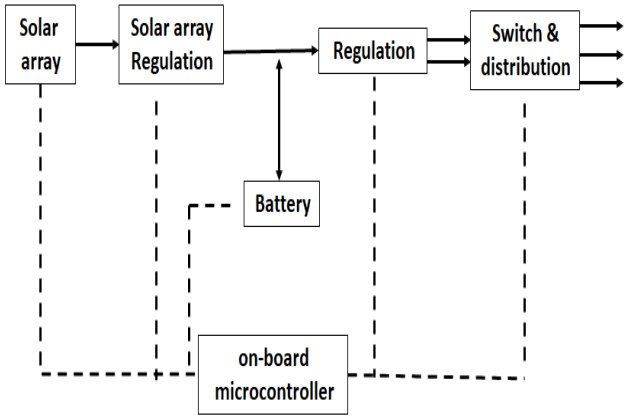

Fig. 1: A standard nano satellite's electrical power system.

The electrical characteristic of a photovoltaic module or array are shown in Figure 2, along with the relationship between output current and output voltage. The output current (I) is controlled by the quantity of solar irradiation, while the output voltage is affected by the temperature of the photovoltaic module/array (V). Manufacturers typically give these I-V characteristic curves [3]. Solar array manufacturers provide a relationship between the array's current and voltage, as well as three locations on the curve. First, MPP, which occurs when the solar array's power output is at its maximum. The following equation can be used to compute the maximum power:

$$P_{max} = I_{mpp} \times V_{mpp} \quad (1)$$

Where $P_{max}, I_{mpp}, V_{mpp}$ are power, current and voltage at the maximum power point respectively.

The open circuit voltage (V_{oc},0) is the second point to consider. When the output terminals of a certain array/module are not connected to any load, this point reflects the maximum voltage of the array/module. This

ISSN No:-2456-2165

open circuit voltage is higher than MPP (V_{mpp}), and it is determined by the number of PV modules/cells connected to form an array/module structure. The third point is the short circuit point (0, I_{sc}), where I_{sc} is the short-circuit current value, which is the maximum current that can be produced by the particular array/module when the output terminals are shorted together. This magnitude of short circuit current is higher than the array/I_{mpp}, module's and the array/module structure is formed by a number of parallel connected modules/ cells.

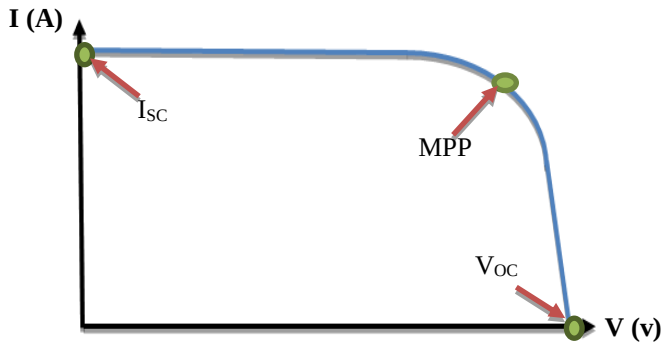

Fig. 2: Actual solar array's characteristics.

II. MAXIMUM POWER POINT TRACKING (MPPT) ALGORITHMS

Maximum power point tracking (MPPT) algorithms are used to increase the power delivered from the solar array. The main procedure of the MPPT algorithm is to adjust the solar array output voltage such that the array supplies maximum power to the load. This is can be achieved through attaching the solar array to a suitable power electronic converter to maximize the solar array developed power. Several MPPT algorithms are suggested by researchers. MPPTs work by connecting the solar array to the battery unit with a switch mode DC-DC converter and keeping the solar array's operational point at the MPP. It accomplishes this by dynamically adjusting the voltage operating point of the solar array, allowing it to swing up to the MPP, where it transforms the input power to the equivalent output power, but at a different voltage and current [4, 5]. The famous one is Perturb and Observe (PAO) or (P&O) algorithm.

The Perturb and Observe method has a simple structure with few measured signals. Through periodic perturbing (may be incrementing or decrementing), the duty cycle of the power switching device is adjusted as shown in Figure 3. Based on the difference between measured output power of the solar array with the output power of the previous perturbation cycle and the voltage derivative, the movement of the new duty cycle is decided. This low-cost technique can be easily designed and implemented [6, 7].

Any spacecraft that uses solar arrays as its major power source needs a way to store energy during eclipse times and peak power demands, which batteries provide. Nickel-metal hydride (NiMH), lithium-ion (Li-ion), and Li-ion polymer are among the battery technologies available (LiPo). Because of their high volumetric and gravimetric energy densities, resulting in a compact, flat battery design with a low magnetic signature, Li-ion or LiPo batteries are the only battery technologies that are practical for nano satellite deployment [8]. They must, however, be used under specific circumstances.

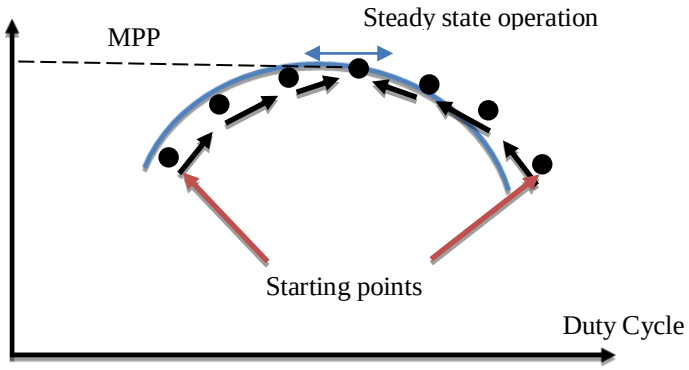

Fig. 3: PAO MPPT algorithm.

The output power is calculated by changing the duty cycle and multiplying the DC-DC converter output voltage and current. The resulting value is then compared to the prior power value to see if the power grew or reduced as a result of the duty cycle change. The duty cycle perturbation is repeated if the output power has risen. If it had dropped, the direction of perturbation would have been reversed [9]. The cycle continues in an endless loop as a new power measurement is taken and compared to the previous one as that shown in Figure 3. The MPPT comprises of a boost DC-DC converter and related control circuitry, with the solar panel as input and the battery unit as output, as shown in Figures 4 and 5. The P&O method is implemented in both analog (Fig. 4) and digital (Fig. 6) form by the control circuits. A microcontroller (MCU) can track the MPP more effectively and perform enhanced versions of the algorithm while being easily tunable, but it is more subject to radiation damage failure. The analog implementation serves as a backup because its discrete circuitry is more resilient than a microcontroller, and the satellite will still be able to operate even if the microcontroller fails. It can also be observed in Figs. 4 and 6 that just the output current, not the output voltage, is being measured. The output voltage can be regarded constant between samples because it is clamped to the slowly changing battery voltage. As a result, just the output current indicates whether power is increasing or decreasing, and only this needs to be measured [10]. Also, because the output of the DC-DC converter is slaved to the battery voltage, a change in duty cycle changes the DC-DC converter input voltage, allowing the solar array's output power to be adjusted [11].

III. ANALOG PAO ALGORITHM

The analog circuitry used to implement the PAO algorithm shown in Fig. 4. The current (or voltage) load value is fed to the analog PAO controller to calculate the maximum power voltage by using MPP calculator [12]. A block diagram of MPP calculator is shown in Fig.5 which searches the maximum power point of the solar array and calculate the maximum power voltage. An input signal to the MPP calculator is sampled and store by using a simple (sample and hold circuit), then it output value compared with

ISSN No:-2456-2165

the stored value to get the change of input signal. Then the logic circuit (consist of XNOR operation and D-flip flop) will find the direction of perturbation. At the end RC charge circuit will charge and discharge capacitor depend on the logic circuit output. When the signal receive from the logic circuit is LOW the capacitor will discharge the maximum power voltage to fall down, and the opposite scenario when the signal receive from logic circuit is HIGH.

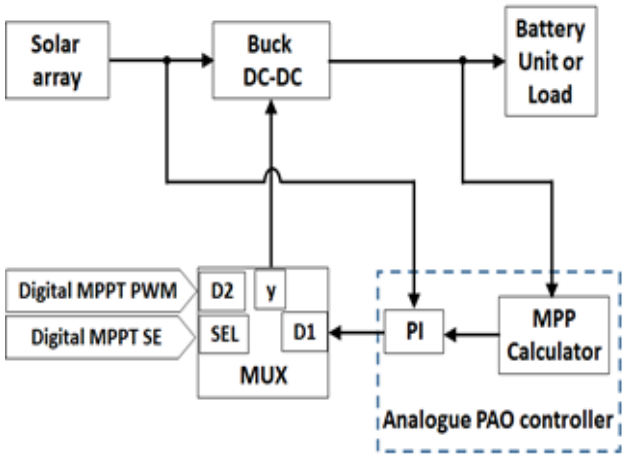

Fig. 4: The analog PAO MPPT algorithm.

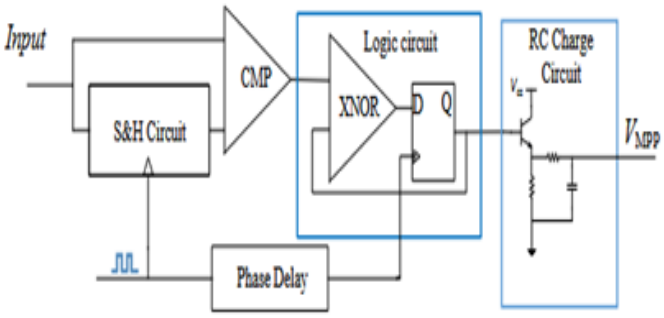

Fig. 5: MPP calculator circuit for analog PAO MPPT algorithm

IV. DIGITAL PAO ALGORITHM

The PAO method is implemented as a logic sub-routine on a microcontroller in the digital MPPT control system depicted in Fig. 6. The fundamental idea is to use the digital version as the primary MPPT controller, with the analog version serving as a backup. A multiplexer (MUX) (as shown in Figs. 4 and 6) handles the MPPT's switchover between digital and analog control, routing the selected pulse width modulation (PWM) signal to the DC-DC converter's MOSFET driver. When the EPS starts on, the MUX's control line is passively pulled LOW, switching to the analog control by default. The MUX control line must be pulled to check that the MCU has started up correctly and is capable of taking control of the MPPT HIGH. An STM32 microcontroller used to made the digital PAO algorithm. A control stage made with a digital microcontroller from STMicroelectronics, with a 32-bit STM32 family, with a good ability for control a power switching supply.

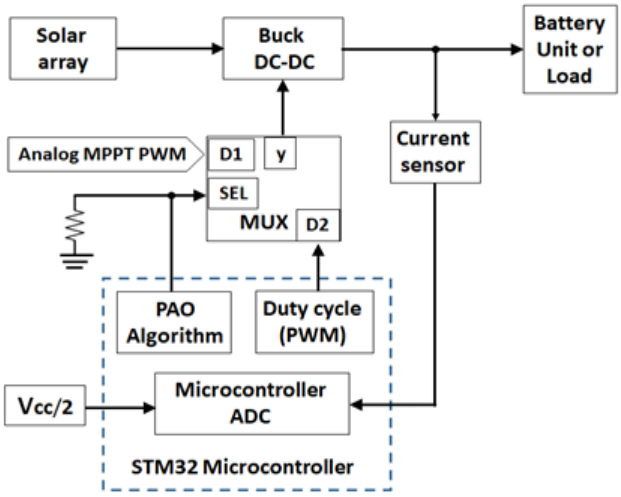

Fig. 6: The digital PAO MPPT algorithm.

V. OVER ALL PROPOSED SYSTEM

A real picture of the proposed hybrid MPPT PAO algorithm is shown in Fig. 7. To valid the proposed prototype this PCB prototype is connected to a solar array that has electrical characteristics as shown in the Fig. 8. The power classes of the used solar array have a wide and very good range to get it in the Lab. also with an artificial light source. An excellent result with an accepted loss are got from the digital algorithm with a good efficiency as that shown in the Table I.

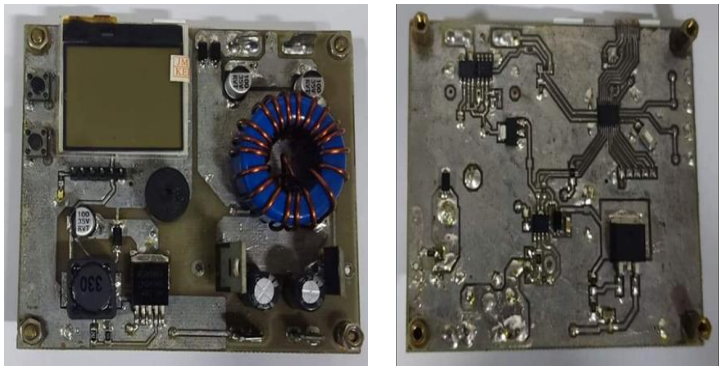

Fig. 7: A proposed prototype of a hybrid MPPT PAO algorithm.

Power Class	245 W	250 W	255 W	260 W	265 W	270 W
Maximum Power (P_{max})	180 W	184 W	187 W	191 W	196 W	199 W
Open Circuit Voltage (V_{oc})	35.0 V	35.1 V	35.4 V	35.7 V	35.9 V	36.1 V
Short Circuit Current (I_{sc})	6.97 A	7.05 A	7.16 A	7.26 A	7.37 A	7.45 A
Voltage at Maximum Power (V_{mpp})	27.8 V	28.0 V	28.2 V	28.4 V	28.6 V	28.7 V
Current at Maximum Power (I_{mpp})	6.48 A	6.54 A	6.64 A	6.73 A	6.84 A	6.92 A
Module Efficiency (%)	13.5 %	13.7 %	14.0 %	14.3 %	14.7 %	14.9 %

Fig. 8: Electrical characteristics of a solar array that used.

ISSN No:-2456-2165

Case	P_{max} (data sheet)	P_{max} (practical) / W	Efficiency
Case I	180	173.21	96.22%
Case II	187	178.88	95.66%
Case III	199	188.73	94.84%

Table 1: Practical results for the proposed digital MPPT.

Table II shows the results of the proposed analog MPPT, with satisfactory efficiency levels of 90.54% under low insolation (245 W) and maintained at 93.36% at large insolation (270 W). This is on average 4.3% less than the digital MPPT, qualifying it as a robust back-up solution. Fig. 9 shows the error in graphic points between the standard solar array MPP values and the values of them that get from our proposed two MPPT algorithms (digital and analog PAO).

Case	P_{max} (data sheet)	P_{max} (practical)	Efficiency
Case I	180	168.06	93.36%
Case II	187	175.23	93.7%
Case III	199	180.17	90.54%

Table 2: Practical results for the proposed digital MPPT.

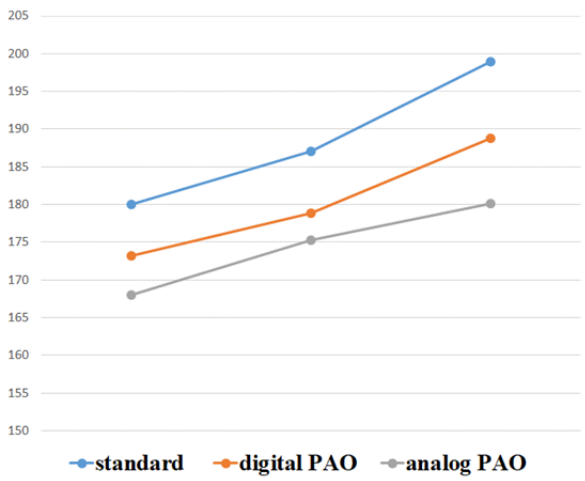

Fig. 9: MPP values for: standard solar array, digital PAO, analog PAO MPPT.

VI. CONCLUSIONS

A prototype of a hybrid MPPT was produced at a different conditions based on a dc-dc buck converter, it designed and implement by using two MPPT algorithms (digital and analog) based on PAO. The first unit (i.e. digital PAO MPPT) represent as a main MPPT unit that enough stand alone to make an excellent maximum power point tracking with high efficiency about 95.57% (as average). And the second unit (analog PAO MPPT) is designed to be as a backup unit to the main MPPT unit, if a failure happened with microcontroller operation. The efficiency of the backup unit (analog PAO) is about (92.53%) and its less than main MPPT unit (digital PAO). For future work multiple parallel dc-dc converters could be used for make independent digital and analog MPPT units. Also a Fuzzy logic controller or neural networks or any artificial intelligence techniques could be used to improve a control specification instead of the traditional PI controller.

REFERENCES

[1.] Toorian, K. Diaz, and S. Lee, “The cubesat approach to space access," in Proceedings of the 2008 IEEE Aerospace Conference. New York, pp. 1-14, 2008.
[2.] J. Stark, Spacecraft Systems Engineering, 3rd ed. West Sussex: Wiley, 2003, pp. 325-354.
[3.] Alternative Energy Tutorials, "Solar Cell I-V Characteristic," 2014. [Online]. Available:http://www.alternative-energy-tutorials.com/energy-articles/solar-cell-i-v-characteristic.html.
[4.] D. Hohm and M. Ropp, “Comparative study of maximum power point tracking algorithms," Progress in Photovoltaics: Research and Applications, vol. 11, no. 1, pp. 47-62, November 2002.
[5.] J. McDermott, Space Mission Analysis and Design, 3rd ed. New York, NY: Springer, 2007, pp. 407-427.
[6.] E. Kroutoulis, K. Kalaitzakis, and N.C. Voulgaris, "Development of a Microcontroller-Based, Photovoltaic Maximum Power Tracking Control System," IEEE Transactions on Power Electronics, vol. 16, no. 1, January 2001.
[7.] L. Piegari, R. Rizzo, "Adaptive perturb and observe algorithm for photovoltaic maximum power point tracking," IET Renewable Power Gener., vol. 4, no. 4, pp. 317-328, Jul 2010.
[8.] V. McLaren, C. Clark, E. Simon, and B. Hendel, “Lithium ion polymer cell for small satellites," in Proceedings of the 2008 NASA Aerospace Battery Workshop . NASA, 2008.
[9.] D. Hohm and M. Ropp, “Comparative study of maximum power point tracking algorithms," Progress in Photovoltaics: Research and Applications, vol. 11, no. 1, pp. 47-62, November 2002.
[10.] K. Lee, J. Niu, and G. Lin, “A simplified analog control circuit of a maximum power point tracker," in Conference Record of the 33rd IEEE Photovoltaic Specialists Conference (PVSC '08) . New York, 2008, pp. 1-3.
[11.] D. Snyman and J. Enslin, “Simplified maximum power point controller for pv installations," in Conference Record of the 23rd IEEE Photovoltaic Specialists Conference (PVSC '93) . New York, 1993, pp. 1240-1245.
[12.] Wang, M. Chen, X. Zhang and M. Gao, "An analog MPPT controller without multiplier for PV applications based on simplified P&O method," 2017 IEEE Energy Conversion Congress and Exposition (ECCE), 2017, pp. 2296-2300, doi: 10.1109/ECCE.2017.8096446.